

ADVANCED PHASES OF EVOLUTION IN MASSIVE RED SUPERGIANTS

RICHARD STOTHERS AND CHAO-WEN CHIN

Goddard Institute for Space Studies, NASA, New York

Received 1969 February 28; revised 1969 July 7, and in proof September 29

ABSTRACT

Very general models have been constructed for the advanced phases of evolution in massive stars of 15, 30, and 60 M_{\odot} . Independent of the surface condition and the specification of the central energy source, the models may be specified by the two quantities E and T_c . Introduction of the physical boundary conditions shows that the models represent evolutionary sequences of convective red supergiants. The phases of carbon, neon, and oxygen burning in the stellar core are considered, with and without the inclusion of the hypothetical electron-neutrino processes. Two starting core compositions are chosen: (1) pure carbon and (2) pure oxygen. Limitations on the possible structure and lifetime up to the presupernova stage are determined. During core carbon burning in the star of 15 M_{\odot} , the core mass increases slightly, while above $\sim 20 M_{\odot}$ and during the later phases of 15 M_{\odot} , the core evolves with monotonically shrinking mass due to the deepening convective envelope. Products of the burning of hydrogen, helium, and carbon are mixed to the surface through the hydrogen-burning shell at the base of the envelope.

Three tests of the hypothesis of electron-neutrino interaction have been made by comparing our theoretical results with the relevant observational data on the statistics of M supergiants, N and S stars, and yellow supergiants. The agreement between the results of all three tests points strongly toward the existence of the postulated interaction.

I. INTRODUCTION

The very advanced phases of evolution have never been explored in realistic models of stars with convective envelopes. The only partial exception is the initial phase of carbon burning in stars of 4 and 15.6 M_{\odot} studied by Hayashi and his associates (Hayashi and Cameron 1962*a, b*; Hayashi, Hōshi, and Sugimoto 1962; Hayashi 1966; see also Masevich *et al.* 1965). A number of idealized structures, intended to represent the cores of evolved stars or stars which have lost their hydrogen-rich envelope, have also been studied (Reeves 1963; Stothers 1963*a*; Fowler and Hoyle 1964; Deinzer and Salpeter 1965; Masani, Gallino, and Silvestro 1965; Chiu 1966; Noels-Grötsch, Boury, and Gabriel 1967; Rakavy, Shaviv, and Zinamon 1967; Kutter and Savedoff 1967; Arnett 1968*b*; Bautz 1968; Faulkner 1968; Fraley 1968; Gabriel and Noels-Grötsch 1968; Masani *et al.* 1968; Sugimoto *et al.* 1968; Beaudet and Salpeter 1969).

It is the intent of this paper to investigate in the broadest sense possible the advanced phases of evolution in stars of high mass. In particular, limitations on the possible structure and lifetime up to the presupernova stage with and without neutrino emission will be determined. Because this is basically an exploratory survey, the adopted approach will be simple but realistic, and the possible uncertainties will be carefully assessed. A number of important comparisons with observational data will conclude the paper; these include *three tests of the hypothesis of electron-neutrino interaction*.

II. BASIC STRUCTURE AND ASSUMPTIONS

The phases of evolution considered in this paper comprise the burning of carbon, neon, and oxygen in the stellar core. The "internuclear" phases of core contraction are also considered, but not in detail. The masses taken to be representative of massive stars are 15, 30, and 60 M_{\odot} , with the zero-age chemical composition assumed to be $X = 0.70$, $Y = 0.27$, and $Z = 0.03$. A schematic H-R diagram is provided in Figure 1 for the purpose of orientation.

The structure of a red supergiant of high mass at the onset of core carbon burning is

not a priori obvious. However, we have for guidance previous work on $1.45 M_{\odot}$ (Rose 1969), $4 M_{\odot}$ (Hayashi *et al.* 1962), $5 M_{\odot}$ (Kippenhahn, Thomas, and Weigert 1966; Weigert 1966), and $15.6 M_{\odot}$ (Hayashi *et al.* 1962). At high mass, self-consistent solutions for carbon burning and later phases may be obtained without calculating in detail the preceding phases of core contraction. The reasons are that the developing convective envelope moves monotonically inward in mass fraction and that the depletion of nuclear fuel is everywhere small on account of the short time scale of contraction. Both of these assumptions have been checked afterward by supplementary calculations, as explained in § V.

Since we have available for our chosen masses the previous evolution up through the exhaustion of helium in the core (Stothers 1963*b*, 1964, 1965, 1966*a, b*; Stothers and Chin 1968), the total abundance and distribution of each main nuclear species may be regarded as known. With these data, we have found the following structure for the phases of carbon burning through oxygen burning: (1) an outer convective envelope, extending

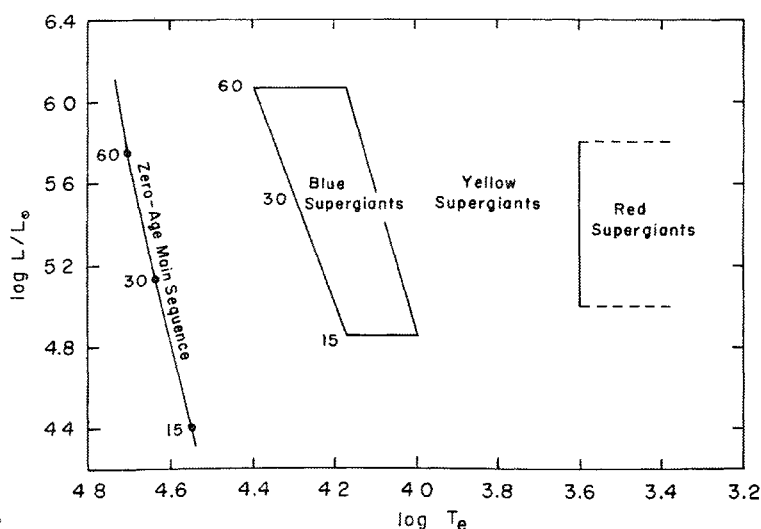


FIG. 1.—Theoretical H-R diagram for massive stars ($15\text{--}60 M_{\odot}$). Core helium burning begins in the red-supergiant region and ends in the blue-supergiant region. Models converge during core carbon burning and later phases in the red-supergiant region.

below the old hydrogen-burning shell; (2) an intermediate radiative zone, containing one or two subzones of homogeneous composition: a carbon-oxygen zone near the convective core and, in some cases, a helium zone just below the convective envelope; (3) an inner convective core. Hydrogen or helium is found to be burning in a thin shell at the base of the convective envelope or at the base of the helium zone, respectively. In most cases, however, the helium zone is absent on account of the extreme depth of the convective envelope. The central nuclear and neutrino processes are confined to the convective core.

We have adopted the customary notations in this paper. In particular, the physical variables of stellar structure have been cast into nondimensional form by using the Schwarzschild (1958) transformations. The following subscripts should be noted: *a*, inner boundary of the convective envelope; *c*, center; *e*, surface; *f*, boundary of the convective core; *g*, gravitational; *s*, shell; H, hydrogen; He, helium; C, carbon; O, oxygen; Ne, neon; and *Z*, heavy elements.

To calculate the structures, we have made the following assumptions and approximations.

1. Rotation and mass loss are neglected.
2. Convective regions are assumed to be rapidly mixed by turbulence, which maintains a steady homogeneity of chemical composition. Penetrative convection at convective-radiative interfaces is ignored, except at the surface, where we assume that the chemical composition of the outer layers is the same as that of the rest of the envelope, because of overshooting mass motions into the photosphere.
3. The interface between any two regions of differing chemical composition is treated by assuming a discontinuity in chemical composition (as well as in luminosity if a shell is burning). Depletion of hydrogen in a burning shell is assumed to be negligible.
4. The equation of state is represented everywhere by the sum of perfect-gas pressure and radiation pressure:

$$P = P_{\text{gas}}/\beta = k\rho T/\mu H + aT^4/3. \quad (1)$$

The mean molecular weight is given by

$$\begin{aligned} \mu &= 4/(5X - Z + 3) && \text{(hydrogen-helium zones),} \\ \mu &= 1.76 && \text{(core).} \end{aligned} \quad (2)$$

The adopted value of μ in the core is correct to within 3 percent for all the phases considered in this paper.

5. The opacity, use of which is required in the dehydrogenized radiative region below the convective envelope, is given by the Compton formula for pure electron scattering, in the form

$$\kappa = 0.19(1 + 2.0T_9)^{-1}, \quad (3)$$

where $T_9 = T \times 10^{-9}$ (Deinzer and Salpeter 1965).

6. The convective envelope is calculated in the fully adiabatic approximation with zero boundary conditions on temperature and pressure and

$$P = KT^{5/2} \left(1 + \frac{1 - \beta}{\beta} \right) e^{4(1-\beta)/\beta} \quad (4)$$

(Hayashi *et al.* 1962). By transforming to nondimensional Schwarzschild variables, the parameter K is replaced by

$$E = 4\pi G^{3/2} (\mu_e H/k)^{5/2} M^{1/2} R^{3/2} K. \quad (5)$$

The quantity E characterizes the adiabat of the interior-envelope solution and is determined by the overlying superadiabatic layer and atmosphere, which we have ignored. It provides the link between the effective temperature and the luminosity. Because of the uncertainty of the theory of nonadiabatic convection, we have left E and T_e as *free parameters*. The nondimensional structure of the envelope is determined by E and A , where

$$A = (4\pi/3) a G^3 (\mu_e H/k)^4 M^2. \quad (6)$$

Complete envelope solutions have been obtained by Stothers (1969*b*).

7. The rates of nuclear-energy generation and of neutrino loss have been adopted from Reeves (1965). Expressing the various rates in the form

$$\epsilon = \epsilon_0 \rho^\omega T_9^\nu, \quad (7)$$

we find the coefficients and exponents listed in Table 1. Electron-screening corrections will be small and may be neglected for our purposes. It should be noted that Arnett and Truran (1969) derived a carbon-burning rate 30 times smaller than Reeves's rate, while

on the other hand, Stephenson (1966) suggested that the rate might be very much larger. In our applications, we shall use a sequence of rates $\frac{1}{30}$, 1.0, and 30 times Reeves's rate $\epsilon(R)$. Models including neutrino processes have been calculated explicitly only for the carbon-burning phase, for which the photoneutrino process and the pair-annihilation process are the dominant sources of neutrinos; we have assumed $\mu_e = 2$ for the mean molecular weight of electrons in the core. The expressions for the shell luminosity and core luminosity are:

$$\text{shell) } L = \epsilon_s q_s M (\gamma_s - 1)^{-1},$$

$$\gamma = \frac{\omega V}{U} \left(\frac{n + \nu/\omega}{n + 1} + \frac{1 - \beta}{\beta} \frac{n - 3}{n + 1} \right) \quad (\text{radiative}), \quad (8)$$

$$\gamma = \frac{\omega V}{U} \left(\frac{\nu/\omega}{n + 1} + \frac{1}{\Gamma_1} \right) \quad (\text{convective}),$$

and

$$\text{(core) } L = \epsilon_c \left(\frac{3k}{2H} \right)^2 \left(\frac{2}{G^3 a} \right)^{1/2} \left(\frac{1 - \beta_c}{\mu_c^4 \beta_c} \right)^{1/2} \left[\frac{n_c + 1}{(n_c + 3\beta_c - 3)(\omega + 1) + \beta_c \nu} \right]^{3/2}. \quad (9)$$

These expressions have been given by Stothers (1966*a*) and by Hayashi *et al.* (1962), respectively, although they have been slightly modified in the first case. Here n is the effective polytropic index.

TABLE 1
DATA ON NUCLEAR AND NEUTRINO PROCESSES

Process	ϵ_0	ω	ν	$\log E_Z$ (ergs g^{-1})	Main Products
CNO bi-cycle.	$10^{24.5} XX_{\text{CNO}}$	+1	12	18.8	${}^4\text{He}$
Triple α	$10^{14.5} Y^3$	+2	19	17.8	${}^{12}\text{C}$
${}^{12}\text{C} + {}^{12}\text{C}$	$10^{7.4} X_{\text{C}}^2$	+1	30	17.7	${}^{16}\text{O}(\beta)$, ${}^{20}\text{Ne}$, ${}^{24}\text{Mg}$
${}^{20}\text{Ne} + \gamma$	$10^{2.3} X_{\text{Ne}}$	0	54	17.1	${}^{16}\text{O}$, ${}^{24}\text{Mg}$
${}^{16}\text{O} + {}^{16}\text{O}$	$10^{-3.4} X_{\text{O}}^2$	+1	39	17.8	${}^{24}\text{Mg}$, ${}^{28}\text{Si}$, ${}^{31}\text{P}$, ${}^{32}\text{S}$
$\gamma + e^-$	$10^{8.0} \mu_E^{-1}$	0	8	.	$e^- + \nu + \bar{\nu}$
$e^+ + e^-$	$10^{13.9}$	-1	16	.	$\nu + \bar{\nu}$

8. The available nuclear fuel at the onset of each burning phase is still rather uncertain. The CNO abundance which participates in the hydrogen-burning reactions at the base of the envelope depends on the rapidity of conversion of ${}^{12}\text{C}$ and ${}^{16}\text{O}$ into ${}^{14}\text{N}$, and hence on the temperature and thickness of the shell, the rate of convective transport in the envelope, and the overall rate of evolution. These quantities are not known a priori, so we have adopted

$$X_{\text{CNO}} = Z_e/2. \quad (10)$$

The uncertainty in X_{CNO} will make little difference in the models. The core-carbon abundance at the end of helium burning depends on the value assumed for the reduced α -particle width of the 7.12-MeV level in ${}^{16}\text{O}$. The most recent evidence suggests $\theta_{\alpha}^2 = 0.08 \pm 0.04$ (Stephenson 1966; Loebenstein *et al.* 1967; Fowler, Caughlan, and Zimmerman 1967). Using $\theta_{\alpha}^2 = 0.1$, Stothers and Chin (1968) have found $X_{\text{C}} = 0.3$ for masses in the range 15–60 M_{\odot} . The rest of the core composition is mostly oxygen. However, we have decided to consider two extreme cases: (a) initially $X_{\text{C}} = 1$ and (b) initially $X_{\text{O}} = 1$. The abundances of the reaction products of carbon burning are, unfortunately, also uncertain. Earlier work suggested roughly comparable amounts of the main nuclear con-

stituents ^{16}O , Ne^{20} , and ^{24}Mg (Cameron 1959*a*; Reeves and Salpeter 1959; Tsuda 1963), although Reeves (1962) had suggested that only little oxygen would be formed. Recently, Arnett and Truran (1969) have determined that $\Delta X_{\text{O}} \lesssim 0.01$, presumably on account of the revised reaction rate for $^{16}\text{O} + \alpha$. The final abundances do not depend much on temperature (even less on density), and their uncertainties are within the temperature uncertainty of the stellar models. Taking into account the small temperature dependence of the final abundances after carbon burning, we find $X_{\text{Ne}} \sim 0.30$ if the initial composition is pure carbon. The main products of neon photodisintegration are almost equal amounts of ^{16}O and ^{24}Mg (Cameron 1959*b*; Reeves 1962; Tsuda 1963). The photodisintegration of ^{28}Si and subsequent element building into the iron peak can be either exothermic or endothermic, depending on whether ^{56}Fe or ^{54}Fe is the end product, i.e., on how fast the evolution proceeds (Truran, Cameron, and Gilbert 1966, 1968). In the event of a long time scale (low temperature), ^{56}Fe is synthesized and the energy release is 3×10^{17} ergs g^{-1} . The relevant nuclear data up to silicon burning are summarized in Table 1.

III. METHOD OF INTEGRATION

The equations of stellar structure have been cast into nondimensional form, as discussed by Hayashi *et al.* (1962). Integration of the equations has proceeded as follows. Initially, the parameter E and the nondimensional temperature t_{H} at the base of the hydrogen envelope are specified. (For convenience, we have substituted t_{H} for T_e as the second free parameter.) With an estimate of μ_e (which fixes the parameter A), an integration is performed from the surface down to the point $l = t_{\text{H}}$. At this point, two conditions must be met. First, q should have closely approached some asymptotic value (q_{H}), since the homology-invariant U is expected to be very small at the base of the envelope on account of the large central condensation. Second, μ_e should be consistent with the properly mixed abundances of hydrogen, helium, and metals as based on the value of q_{H} . When these conditions are met, the luminosity L is found by equating the radiative and adiabatic effective polytropic indices $n_{\text{rad}} = n_{\text{ad}}$ at the base of the envelope:

$$L = \frac{32\pi cGMq}{0.19(1+X)} \left(\frac{4 - 7\beta + 3\beta^2}{32 - 24\beta - 3\beta^2} \right). \quad (11)$$

At the burning shell(s), a trial estimate of L_s/L is made so that the jump in luminosity can be performed. Simultaneously, the physical temperature of the shell (and hence the effective temperature of the star) is calculated from the formula for the shell luminosity. The integration is then carried to the boundary of the convective core. Trial solutions for the convective core are calculated separately by specifying the effective polytropic index at the center, n_c . Fitting of shell-inward and center-outward integrations is made at the boundary of the convective core in the parameters n , U , and V . The central temperature and the definitive values of the shell temperature(s) and of the effective temperature then follow in a straightforward way.

IV. MODELS WITH BURNING CORES

Models for our chosen masses and for various values of E and T_e are presented in Tables 2-4. The basic structural quantities at a given E -value are nearly independent of effective temperature (usually to within ± 2 in the last significant figure). The burning shells have nearly fixed temperatures: $5-7 \times 10^7$ °K (hydrogen), 2×10^8 °K (helium), and 6×10^8 °K (carbon). On the other hand, the central temperature, and therefore the central density, is very sensitive to effective temperature.

It is important to note that, for specified values of E and T_e , the luminosity, surface chemical composition, and central temperature are uniquely determined. This requires no knowledge about the surface conditions or about the nuclear reactions in the core.

* $\int Xdq = 0.36$; $\int Ydq = 0.25$; italics indicate models with helium-burning shell.

TABLE 4

SELECTED EVOLUTIONARY MODELS FOR 15 M_{\odot} WITH ONE BURNING SHELL*

Variable	$E=9$	$E=10$	$E=11$	$E=11.5$	$E=12$	$E=12.5$	$E=12.7$	$E=13$	$E=14$	$E=18$	$E=24$
X_e	0.69	0.65	0.62	0.61	0.60	0.59	0.59	0.58	0.56	0.51	0.47
Y_e	0.28	0.32	0.35	0.36	0.37	0.38	0.38	0.39	0.38	0.35	0.32
Z_e	0.03	0.03	0.03	0.03	0.03	0.03	0.03	0.03	0.06	0.14	0.21
$\log(L/L_{\odot})$	5.14	5.10	5.08	5.06	5.04	5.03	5.03	5.03	4.99	4.81	4.45
L_s/L_{\odot}	0.69	0.66	0.60	0.60	0.58	0.54	0.51	0.47	0.56	0.77	0.94
q_a	0.36	0.32	0.29	0.28	0.27	0.25	0.24	0.24	0.22	0.14	0.061
q_s	0.24	0.24	0.24	0.24	0.24	0.24	0.24	0.24	0.22	0.14	0.061
q_f	0.11	0.11	0.11	0.11	0.11	0.11	0.11	0.10	0.091	0.048	0.015
β_e	0.76	0.77	0.77	0.77	0.77	0.77	0.78	0.78	0.80	0.87	0.96
$\log(M_f/L_f)$	-4.73	-4.71	-4.77	-4.75	-4.75	-4.78	-4.80	-4.88	-4.79	-4.61	-4.18

$\log T_e$

$\log T_e$:											
3.7	8.74	8.76	8.79	8.82	8.86	8.92	8.95	9.03	8.98	8.99	9.04
3.5	8.77	8.79	8.82	8.86	8.90	8.98	9.04	9.13	9.08	9.08	9.13
3.3	8.80	8.83	8.87	8.91	8.99	9.26	9.17	9.16	9.15	9.16	9.22

* $\int Xdq = 0.44$; $\int Ydq = 0.30$; italics indicate models with helium-burning shell.

TABLE 3

SELECTED EVOLUTIONARY MODELS FOR 30 M_{\odot} *

Variable	$E=2$	$E=2.5$	$E=3$	$E=4$	$E=5$	$E=6$	$E=7$	$E=8$	$E=9$	$E=10$
X_e	0.65	0.58	0.53	0.48	0.44	0.42	0.41	0.40	0.39	0.38
Y_e	0.32	0.39	0.37	0.33	0.31	0.29	0.28	0.27	0.27	0.26
Z_e	0.03	0.03	0.10	0.19	0.25	0.29	0.31	0.33	0.34	0.36
$\log(L/L_{\odot})$	5.59	5.55	5.49	5.38	5.28	5.18	5.08	4.97	4.84	4.68
L_s/L_{\odot}	0.01	0.00	0.11	0.28	0.42	0.53	0.64	0.74	0.82	0.90
q_a	0.44	0.38	0.32	0.24	0.19	0.15	0.12	0.089	0.067	0.047
q_s	0.37	0.37	0.32	0.24	0.19	0.15	0.12	0.089	0.067	0.047
q_f	0.32	0.26	0.21	0.15	0.10	0.074	0.052	0.035	0.023	0.014
β_e	0.52	0.54	0.57	0.63	0.69	0.73	0.78	0.83	0.88	0.93
$\log(M_f/L_f)$	-4.91	-4.96	-4.94	-4.89	-4.86	-4.80	-4.75	-4.67	-4.56	-4.36

$\log T_e$

$\log T_e$:										
3.7	8.58	8.75	8.78	8.80	8.82	8.86	8.90	8.93	8.95	9.00
3.5	8.65	8.82	8.86	8.89	8.92	8.95	8.98	9.01	9.05	9.09
3.3	8.75	8.89	8.94	8.97	9.00	9.03	9.06	9.09	9.11	9.16

We have merely assumed that the region interior to the shell source is being supported against gravitational contraction by some "point source" of energy within the convective core.

In all cases, if E or T_c is held fixed, a decrease of T_c or an increase of E , respectively, leads to a hotter central temperature. An increase of E also leads to a smaller core and therefore to a lower luminosity, because the stellar core behaves like a single star. Since the effective temperature will, at worst, not increase drastically during evolution, the tabulated models actually represent evolutionary sequences in time with increasing central temperature.

An evolutionary stage is determined by the abundance Z of the relevant nuclear fuel in the convective core. This abundance is calculated directly from the equation for the core luminosity (in the case of no neutrino emission) or else from the equation $L_{\text{nuc}} = L_c$, by using the core formula for each luminosity (in the case including neutrino emission).

TABLE 4
SELECTED EVOLUTIONARY MODELS FOR $60 M_{\odot}^*$

Variable	$E=0.2$	$E=0.3$	$E=0.4$	$E=0.6$	$E=0.8$	$E=1.0$	$E=1.2$	$E=1.4$
X_c	0.40	0.37	0.35	0.32	0.31	0.30	0.30	0.29
Y_c	0.35	0.31	0.30	0.28	0.27	0.26	0.25	0.25
Z_c	0.25	0.32	0.35	0.40	0.42	0.44	0.45	0.46
$\log(L/L_{\odot})$..	5.85	5.74	5.66	5.51	5.39	5.27	5.13	4.96
L_c/L_{\odot} .. .	0.00	0.12	0.19	0.34	0.45	0.57	0.68	0.80
q_a	0.31	0.24	0.20	0.14	0.10	0.077	0.056	0.038
q_s	0.31	0.24	0.20	0.14	0.10	0.077	0.056	0.038
q_f	0.23	0.17	0.13	0.086	0.058	0.039	0.024	0.013
β_c	0.45	0.50	0.54	0.61	0.67	0.73	0.79	0.86
$\log(M_f/L_f)$..	-5.01	-4.98	-4.98	-4.92	-4.89	-4.83	-4.78	-4.67
log T_c								
log T_c :								
3.7	8.65	8.69	8.72	8.78	8.83	8.88	8.94	9.00
3.5	8.71	8.75	8.79	8.85	8.90	8.96	9.01	9.07
3.3	8.74	8.81	8.85	8.91	8.97	9.02	9.07	9.13

* $\int Xdq = 0.28$; $\int Ydq = 0.24$.

It is obvious that Z is determined primarily by the central temperature in the core equations. Table 5 contains the relevant temperatures for the burning of various fuels (including fuels burning in a shell). The maximum deviation from these values which occurs in our models is $\Delta \log T = \pm (0.7/\nu)$. Interpolation for any other abundance may be performed with the help of the relation $T \sim Z^{-(1+\omega)/(\nu+3\omega)}$.

In the situations where neon and oxygen burning occur outside the range of our tabulated models (in small, dense cores), we have assumed that the following sequence of events takes place. Gravitational contraction of the core is slowed down by electron degeneracy at some critical core mass which is a function of central temperature (Takarada, Sato, and Hayashi 1966). The star is then in the same situation encountered by red giants of lower mass. The inward growth of the convective envelope ceases when the hydrogen-burning shell becomes virtually the sole source of energy. As the shell burns outward and adds mass to the core, a critical core mass is reached at which a neon or oxygen flash occurs. The flash evolves into a phase of normal burning inside an expanded core (for no neutrino emission) or into a phase of explosive burning (with neutrino emission). The critical core mass for neon or oxygen burning is in the range $1.2-1.4 M_{\odot}$ (Takarada *et al.* 1966; Murai *et al.* 1968).

With this brief introduction, it is now possible to discuss in turn the overall evolution of our models of 15, 30, and 60 M_{\odot} .

a) 15 M_{\odot}

Regardless of its effective temperature, a star of 15 M_{\odot} initiates carbon burning with its original carbon core intact and with a helium shell burning. Consequently, for a while at least, its evolution proceeds much as in the case of 15.6 M_{\odot} considered by Hayashi *et al.* (1962). In the present case, however, the mass of the helium zone is much smaller. This is due to the bigger core formed during the previous evolutionary phases, since Hayashi *et al.* adopted a lighter mean molecular weight for the zero-age composition.

In the case of a *long* carbon-burning phase (large initial carbon abundance and no neutrino emission), the depletion of helium causes the helium shell to approach the inactive hydrogen shell so closely that the hydrogen is reignited and the helium shell becomes correspondingly weakened. Although we have not presented in Table 2 any

TABLE 5
APPROXIMATE NUCLEAR-BURNING TEMPERATURES

REGION	FUEL ABUNDANCE	log T					
		No ν		ν		No ν	
		30 $\epsilon(R)$	30 $\epsilon(R)$	$\epsilon(R)$	$\epsilon(R)$	$\epsilon(R)/30$	$\epsilon(R)/30$
H shell.	X_e	.	..	7.78
He shell...	0.97	.	..	8.30
C shell ...	1.00	8.78
C core. . . .	1.00	8.77	8.79	8.80	8.84	8.85	8.92
C core. . . .	0.03	8.86	8.92	8.91	8.98	8.94	9.04
Ne core. . . .	1.00	9.08
Ne core. . . .	0.03	.	..	9.11
O core. . . .	1.00	..	.	9.09
O core. . . .	0.03	.	..	9.16

models with two shells burning, we have verified that they are very similar to the models presented there without helium depletion. The reason for this is that the extent of depletion is sharply limited by the incursion of the hydrogen convective envelope, the depletion being at most $\Delta \int Y dq \sim 0.03$. Consequently, the core mass (3.6 M_{\odot}) does not grow extensively as in Hayashi's case.

By the onset of neon and oxygen burning in the core, two shells are burning simultaneously—hydrogen and carbon. The inward-moving convective envelope has swamped the old helium shell, and the products of helium burning are mixed to the surface. The carbon shell now takes over the role of the old helium shell. In the carbon shell, however, depletion of carbon may be neglected on account of the short time scale of central neon and oxygen burning. Hence, the mass of the core below the carbon shell (1.7 M_{\odot}) may be taken as constant. Models for the neon-oxygen phase (without neutrino emission) are presented in Table 6. The basic structural quantities at a given E -value are nearly independent of the effective temperature and of the abundance of carbon in the carbon zone, although the ratio of shell luminosities L_H/L_C , the central temperature, and the central density are not.

In the case where the initial composition of the core is pure oxygen, the star initiates oxygen burning inside a small core blanketed by a deep convective envelope. Models with contracting cores (§ V) indicate that this situation obtains only under the condition

that $\log T_e \geq 3.50$ when $E = 12.5$ – 13 , which seems to be a correct condition physically (§ VII).¹

b) 30 and 60 M_\odot

The stars of 30 and 60 M_\odot evolve in the same pattern. The convective envelope extends below the old hydrogen and helium shells, so that hydrogen now burns at the inner edge of a very deep convective envelope. The surface is enriched in helium and in products of former helium burning. If a carbon-burning phase precedes oxygen burning, the products of carbon burning are also mixed to the surface. A carbon *shell*, however, is never ignited, because the inward-moving convective envelope swamps the carbon zone before the temperature is sufficiently hot to burn the carbon. Thus, neon and oxygen burning occur in a structure which is very similar to that found for carbon burning.

TABLE 6
SELECTED EVOLUTIONARY MODELS FOR 15 M_\odot WITH TWO BURNING
SHELLS (HYDROGEN AND CARBON)*

Variable	$E=15$	$E=16$	$E=17$	$E=18$
$(L_H+L_C)/L$. . .	0.66	0.74	0.77	0.78
q_H	0.20	0.18	0.16	0.14
q_C	0.11	0.11	0.11	0.11
q_f	0.071	0.050	0.042	0.038
β_c	0.82	0.85	0.87	0.89
$\log (M_f/L_f)$. . .	-4.74	-4.73	-4.71	-4.69
$\log T_e$	3.50	3.50	3.50	3.50
$X_C(q_C)$	1.00	1.00	1.00	1.00
L_H/L	0.60	0.55	0.50	0.45
$\log T_c$	9.04	9.09	9.14	9.23

* Other basic quantities same as in Table 2

V. MODELS WITH CONTRACTING CORES

A sequence of models with contracting cores can be shown to cause an inward growth of the convective envelope at the onset of core nuclear burning in all our masses. This may be seen qualitatively as follows. For a specified central temperature (i.e., the onset of a core-burning phase), a gravitational source of energy provides a larger core luminosity than does a nuclear source, because of the milder temperature dependence of the rate of energy production in the former case. With the inclusion of neutrino energy losses, this conclusion is true a fortiori (cf. Murai *et al.* 1968; Sugimoto *et al.* 1968). Since a large total luminosity at the position of the shell corresponds to a small E -value in our models, we will have justified our original proposition if the luminosity of the shell itself does not correspondingly decrease during the interior transition from a gravitational to a nuclear-burning source of energy.

To check this, a number of contraction models without neutrino emission have been

¹ An interesting corollary to the Russell-Vogt theorem is provided by this particular situation. For a structure composed of two chemically homogeneous regions of different composition (oxygen in the core and a hydrogen-oxygen mixture in the envelope), two models can be found representing the same stage of evolution when oxygen and hydrogen are simultaneously burning at the center and at the base of the envelope, respectively. The two models contain the same integrated amounts of oxygen and hydrogen and have all their hydrogen confined to the convective envelope, but the distribution of elements does differ in that the fraction of mass contained within the envelope is different in the two cases. A sequence of model pairs can be found by examining the nonmonotonic trend of central temperature with increasing envelope depth in Table 2 (e.g., $E = 13$ – 24 for $\log T_e = 3.5$).

constructed. In these models the nuclear-energy source near the center has been replaced by a uniform source of gravitational-energy release at all points below the nuclear-burning shell, so that

$$\text{(core)} \quad L(q) = \epsilon_g q . \quad (12)$$

The approximation of constant ϵ_g in the core is very well justified in the absence of neutrino processes (Hayashi *et al.* 1962; Murai *et al.* 1968). It may be noted that no new parameters are introduced in the solutions, since

$$\epsilon_g = \frac{(1 - L_H/L)L}{q_s M} . \quad (13)$$

Furthermore, the transfer of gravitational and thermal energy in the convective envelope is irrelevant, since the envelope is in adiabatic equilibrium. Thus, the luminosity L refers strictly to the luminosity at the position of the shell, not at the surface (where L may be smaller or larger). The region below the shell is in radiative equilibrium throughout. The mean molecular weight below the shell is taken to be $\mu_c = 1.76$. For simplicity, the opacity is assumed to be constant and equal to $\kappa = 0.19$. With this approximation, the radiative-core solutions may be cast into nondimensional form with n_c as a parameter, analogous to the convective-core solutions (Hayashi *et al.* 1962). Fitting of the envelope and core is performed as before. For comparison, a number of models with nuclear burning in the core were recomputed with $\kappa = 0.19$.

In all cases, for a given effective temperature, the E -value in the core-contraction model is smaller than the E -value in the core-burning model at the same central temperature. Furthermore, a sequence of contraction models in order of increasing E -value also represents an evolutionary sequence with increasing central temperature. We have thus shown that the inner boundary of the convective envelope moves monotonically inward during the contraction phase up to the onset of nuclear burning in the core. Therefore, the condition $n_{\text{rad}} = n_{\text{ad}}$ to determine the inner boundary of the envelope during the initial phases of nuclear burning in the core is justified.

VI. EVOLUTIONARY LIFETIMES

a) *Burning Cores*

The lifetime for fuel depletion in a convective core is given by

$$\tau = E_Z \int \frac{M_f}{L_f} dZ , \quad \tau_\nu = E_Z \int \frac{M_f}{(L + L_\nu)_f} dZ , \quad (14)$$

for the case without and the case with neutrinos, respectively. These expressions may be evaluated readily with the help of Tables 1–6 and equation (9).

Since the effective temperatures of highly evolved red supergiants are uncertain, we may obtain a *minimum* lifetime for each phase by choosing the smallest possible M_f/L_f ratio. For the case without neutrino emission, this corresponds to taking the lowest realistic effective temperature ($\log T_e = 3.3$), holding it constant, and letting the E -value decrease. For the case including neutrino emission, such a procedure results in a *maximum* lifetime for the following reason. The neutrino luminosity L_ν depends essentially only on the central temperature. Since $(L + L_\nu) \approx L_\nu$ and since the lowest effective temperature yields the largest core mass, the ratio $M_f/(L + L_\nu)_f$ is maximized by choosing the lowest effective temperature.

The case of $15 M_\odot$ is rather special. Here the lifetime is nearly independent of effective temperature if $X_C = 1$ initially; the reason is that the nuclear-burning shells are practically *fixed* in mass fraction during evolution (the core mass is constant). We shall use $\log T_e = 3.5$ for the two initial cases, $X_C = 1$ and $X_O = 1$.

To simplify the argument further in the case without neutrino emission, we shall formally consider carbon burning as resulting in the formation of pure silicon; i.e., we shall lump together the various burning phases from ^{12}C to ^{28}Si . We shall likewise consider ^{16}O as going only into ^{28}Si when the core is assumed initially to be composed of pure oxygen. These simplifications preserve the minimization of the lifetime, since the \dot{M}_f/L_f ratio increases slightly during evolution. With the new values of $E^*_\text{C} = 7.4 \times 10^{17}$ ergs g^{-1} and $E^*_\text{O} = 4.6 \times 10^{17}$ ergs g^{-1} , we obtain the lifetimes listed in Table 7.

TABLE 7
MINIMUM LIFETIME WITH NO ν AND MAXIMUM LIFETIME WITH ν
FOR CARBON AND OXYGEN BURNING (10^5 years)

INITIAL COMPOSITION OF CORE AND RATE	15 M_\odot		30 M_\odot		60 M_\odot	
	No ν	ν	No ν	ν	No ν	ν
$X_\text{C}=1$:						
30 $\epsilon(R)$	4.4	0.45	2.9	0.20	2.7	0.20
$\epsilon(R)$	4.2	0.10	2.8	0.032	2.7	0.046
$\epsilon(R)/30$	4.3	0.019	2.8	0.0075	3.0	0.0098
$X_\text{O}=1$:						
$\epsilon(R)$	6.5	<0.2 yr	4.3	<0.2 yr	3.2	<0.2 yr

TABLE 8
MINIMUM LIFETIME OF CORE CONTRACTION FROM END OF HELIUM
BURNING TO ONSET OF CARBON/OXYGEN BURNING (10^4 years)*

CORE COMPOSITION AND RATE	15 M		30 M_\odot		60 M_\odot	
	No ν	ν	No ν	ν	No ν	ν
$X_\text{C}=1$						
30 $\epsilon(R)$	1.4	1.1	0.5	0.4	0.2	0.2
$\epsilon(R)$	1.5	1.1	0.6	0.5	0.2	0.2
$\epsilon(R)/30$	1.9	1.2	0.7	0.5	0.3	0.2
$X_\text{O}=1$						
$\epsilon(R)$	3.7	1.2	1.3	0.5	0.5	0.2

* Based on core masses of 3.6, 11, and 28 M_\odot , respectively.

The lifetime of oxygen burning in the presence of neutrino emission has been interpolated from the results of Rakavy *et al.* (1967), since our simple core structures are not valid in this case.

b) Contracting Cores

We have not calculated the lifetime of the contraction phases. However, limits on the lifetime may be obtained from the results of Murai *et al.* (1968), who considered the contraction phase of stars with constant mass and uniform composition ($\mu = 1.75$). A lower limit on the lifetime is obtained by choosing the contracting mass as constant and equal to the original mass of the core inside the old helium shell, which is 3.6 M_\odot (for 15 M_\odot), 11 M_\odot (for 30 M_\odot), and 28 M_\odot (for 60 M_\odot). (An upper limit is analogously derived by using the *final* mass of the core at the onset of carbon or oxygen burning.) The initial temperature is taken to be that found at the end of core helium burning ($T_c = 3 \times 10^8$ °K). Results for the *minimum* lifetime are listed in Table 8.

VII. DISCUSSION OF INITIAL ASSUMPTIONS

a) *Surface Condition*

Hayashi and Cameron (1962*a*) demonstrated that a star of $15.6 M_{\odot}$ has a tremendously extended envelope at the onset of carbon or neon burning if the envelope is assumed to be in radiative equilibrium, and hence that a surface convection zone must be taken into account. We have also tried radiative-envelope solutions (with hydrogen- and/or helium-burning shells) for our masses, with the same result. This is basically a consequence of the very large central condensation induced after core helium exhaustion by (1) the large difference in mean molecular weight between core and envelope and (2) the high temperature of the core. We have inferred that our structures are uniquely determined.

To demonstrate quantitatively the validity of the convective-envelope assumption, we have used the mixing-length theory of convection for the outer layers, as coded in a computer program kindly loaned to us by I. Iben, Jr., and described elsewhere (Iben 1963). Given L , T_e , and the chemical composition of the envelope, it is possible to determine E from this program. Since the program treats the ionization of metals incompletely, it is strictly valid only for the carbon-burning models of $15 M_{\odot}$, where Z_e is small. For these models with $\bar{E} = 9-13$, we find $\log T_e = 3.57-3.58$ by using a ratio of mixing length to density scale height equal to 0.5. Furthermore, even despite our neglect of the extensive contribution to ionization by the CNO elements in the remaining models of Tables 2-4, we have verified that the surface layers are indeed convective in all cases.

b) *Mixing into Radiative Zone*

If mixing between the convective envelope and the inner convective core is able to occur, the star will become chemically homogenized. Two types of mixing may occur: (1) penetrative convection and (2) rotationally induced currents. The importance of type 1 is ruled out by the large number of density scale heights occurring in the radiative zone, ranging, from a *minimum* of eight at the onset of carbon burning to a much larger number as the core mass decreases. Type 2 is also unimportant on the following grounds. If the star originally reached the upper main sequence in approximately rigid rotation (Sugimoto *et al.* 1968), having a typical equatorial velocity of 200 km sec^{-1} (Allen 1963), then the ratio of centrifugal force to gravity at the equator, χ , must have been 0.06 ($15 M_{\odot}$), 0.05 ($30 M_{\odot}$), or 0.03 ($60 M_{\odot}$). Rotational mixing is negligible in this case (Schwarzschild 1958). During the subsequent evolution, if each mass shell in the star conserves its angular momentum, the ratio of forces at the core boundary is found to remain nearly as small. In the most extreme case of a degenerate core mass of $1.2 M_{\odot}$, the ratio of centrifugal force to gravity is less than 0.10; this corresponds to a rotational mixing time of the order of $(GM^2/\chi RL)_s = 3 \times 10^6$ years, which is far longer than the relevant evolution time. We conclude that massive supergiants must evolve with cores essentially structured as we have assumed them to be.

c) *Shell Thickness*

The thickness of a burning shell may be obtained directly from the expression for the shell-luminosity fraction,

$$L_s(q)/L_s = 1 - (q/q_s)^{1-\gamma_s}. \quad (15)$$

For $\gamma_s \gg 1$, we have

$$(\Delta \ln q)_s = \gamma_s^{-1}, \quad (\Delta \ln x)_s = \gamma_s^{-1} U_s^{-1}. \quad (16)$$

A burning shell is characterized typically by $V \approx n + 1 \approx 4$ and $\Gamma_1 \approx \frac{4}{3}$; consequently, $\gamma_s \approx (\nu + 3\omega)/U_s$. Since U and x are generally quite small at a shell, the mass and

thickness of the shell are also small. Consequently, the approximation of a simple discontinuity in L at a burning shell is well justified in our models, since $(\Delta q)_s$ and $(\Delta x)_s$ are approximately 10^{-5} and 10^{-5} (hydrogen shell) and 10^{-3} and 10^{-6} (helium shell), respectively.

d) Depletion of Hydrogen and Helium

The depletions of hydrogen and helium during evolution may be calculated from

$$\Delta \int X dq = - \frac{\int L_H dt}{E_H M}, \quad \Delta \int Y dq = - \frac{\int L_{He} dt}{E_{He} M}. \quad (17)$$

The depletion of helium occurs only during the carbon-burning phase of $15 M_\odot$ and has been discussed earlier (§ IV). The depletion of hydrogen is negligible ($\Delta \int X dq \leq 0.01$) in all phases up to supernova explosion if neutrino losses are included. In the absence of neutrino losses, it is always negligible for carbon burning, although it is negligible for oxygen burning only if the lifetime is short, i.e., if the effective temperature is low. Our initial assumption that $\Delta \int X dq$ may be neglected is therefore justified, since we have adopted low effective temperatures.

e) Opacity and Electron Degeneracy

Less than 15 percent of the opacity at the inner edge of the convective envelope is found to be contributed by bound-free absorption in all the models of Tables 2-4. Hence, our adoption of solely electron scattering in equation (11) is justified. The degeneracy parameter Ψ at the center of our models never exceeds ~ 1 and is usually much smaller. Therefore, our adopted equation of state is quite adequate to represent the pressure.

f) Zero-Age Chemical Composition

The quantitative effect of a somewhat different choice of initial chemical composition ought to be small. Certainly, no qualitative change in our results is expected. For example, Hayashi *et al.* (1962) used $X_e = 0.90$ and $Z_e = 0.02$ in their evolutionary sequence for $15.6 M_\odot$. The core mass during most of the carbon-burning phase was $\sim 3.6 M_\odot$, virtually the same as for our $15 M_\odot$ sequence.

g) Mass Loss

Mass loss, as long as it is confined to removal of the material in the envelope, has virtually no effect on the stellar luminosity or lifetime if the core mass is fixed (Hayashi *et al.* 1962; Forbes 1968). It does, however, lower the effective temperature unless the envelope mass becomes very small. Since the core mass is not fixed in most of our model sequences, we have based our lifetime calculations in Table 7 on the *maximum* possible core mass, i.e., on those cases where the convective envelope is smallest. Consequently, mass loss should not be an important factor in our comparisons. Certainly, *sudden* loss of the envelope due to dynamical instability is not indicated for massive stars, according to theoretical models (Paczynski and Ziolkowski 1968) and the observational fact of very low effective temperatures in luminous M and N stars. Moreover, the observed rate of *steady* mass loss from the red supergiant α Ori ($\sim 25 M_\odot$) is rather ineffectual, with estimates ranging from 1.5×10^{-8} to $4 \times 10^{-6} M_\odot \text{ year}^{-1}$ (Deutsch 1956; Wilson 1960; Weymann 1962).

VIII. SUPERNOVAE

a) Core Mass

Under the influence of neutrino emission, the cores of our models will undergo a rapid contraction after carbon burning, which is scarcely interrupted by the later burning

phases (Reeves 1963; Stothers 1963*a*). As explained in § V, the convective envelopes will not be nearly so deep as indicated for the central temperatures of the *static* models in Tables 2–4. The time required to radiate or convect away the heat content of the outer portion of the core is simply too long compared with the neutrino evolution time. (We are indebted to D. Sugimoto for pointing this out to us.) In order to estimate *minimum* values for the final core masses, we have adopted a central temperature of 10^9 °K; at this temperature the static-core approximation should certainly have reached the limit of its validity. The resulting values for the minimum core masses are entered in Table 9. In all cases, they exceed the Chandrasekhar mass limit, and the stars are expected to become implosion-type supernovae.

In the absence of neutrino emission, the rate of evolution up to silicon ignition is certainly sufficiently slow to permit the deep incursion of the convective envelopes as indicated by Tables 2–4. The final core masses at the supernova stage will be approximately equal to the Chandrasekhar mass limit, $\sim 1.4 M_{\odot}$. A detailed treatment would be required to say whether a detonation-type or an implosion-type supernova event occurs. But it is possible that, if a significant carbon abundance results from core helium burning and if Urca neutrino processes are effective in collapsing the core after oxygen burning, the final core masses in stars of 10 – $20 M_{\odot}$ would exceed the Chandrasekhar mass limit

TABLE 9
LOWER LIMIT ON THE CORE MASS (M_{\odot}) AT ONSET
OF THE SUPERNOVA STAGE BASED ON MODELS
WITH NEUTRINO EMISSION

$\log T_e$	$15 M_{\odot}$	$30 M_{\odot}$	$60 M_{\odot}$
3.7...	3.6	1.4	2.3
3.5 ..	3.6	3.0	3.6
3.3 ..	3.6	5.7	5.2

(see Table 6 and Arnett [1968*b*]). Then an implosion would be expected to occur in stars of this mass range.

b) Envelope Ejection

Detailed supernova models (assuming constant mass before explosion) have been calculated by Colgate and White (1966), Colgate (1968), and Arnett (1967, 1968*a,b*) for chemically homogeneous structures of 1 – $32 M_{\odot}$ representing cores of evolved stars. Although the structures with masses greater than 4 – $10 M_{\odot}$ may not eject matter, at least 10^{51} ergs of kinetic energy are always available in the structures of lower mass. This is more than enough to remove the convective envelopes of our models, whose gravitational potential energy is, at the very most, 10^{49} ergs ($15 M_{\odot}$), 5×10^{49} ergs ($30 M_{\odot}$), and 10^{50} ergs ($60 M_{\odot}$). In fact, if $\log T_e = 3.3$, these numbers should be reduced by a factor of about 10.

IX. THREE TESTS OF THE NEUTRINO HYPOTHESIS

Three tests of the hypothesis of electron-neutrino interaction can be made with the results obtained in the present paper. On the observational side, all three tests require information on stellar statistics. From the theoretical point of view, this information must be interpreted by using lifetimes calculated with and without the inclusion of neutrino-emission processes. It will become clear that only *lower limits* on lifetimes without neutrino emission are required to make the tests valid. Therefore, we may simply consider the phases of carbon-to-silicon burning in the stellar models.

It is important to note that the Urca neutrino process, which does not depend on the

hypothetical electron-neutrino interaction, is *irrelevant* in the present context, since it becomes important only during the advanced phases of silicon-to-iron burning (Chiu 1961, 1963; Hayashi *et al.* 1962; Dallaporta and Saggion 1968). Thus, it will have no effect on our observational comparisons.

a) *Statistics of M Supergiants*

The observed numbers of blue and red supergiants have been compared in a previous paper (Stothers 1969*a*) with the theoretical lifetimes of these stars. Only members of young clusters and associations were considered, since (1) red supergiants in the general field can be derivatives of all masses along the main sequence, (2) the (initial) masses of red supergiants can be estimated to be virtually the same as those of blue supergiants in the same cluster, and (3) a 1-to-1 correspondence between mass and luminosity exists for the blue supergiants. As discussed in Stothers (1969*a*), only the observational data relating to clusters containing the *most massive* stars are unambiguous and therefore applicable to a test comparing the numbers of OBA and M supergiants. Hayashi and his associates (Hayashi and Cameron 1962*b*, 1964; Hayashi *et al.* 1962) originally made this test in the case of the I Per association and came to a negative conclusion about the

TABLE 10
OBSERVED NUMBER OF SUPERGIANTS IN CLUSTERS CONTAINING RED
AND BLUE SUPERGIANTS OF HIGH MASS*

Cluster	$M_{\text{blue}}/M_{\odot}$	Median $M_{\text{blue}}/M_{\odot}$	Blue n_b	Red n_r	n_b/n_r
I Ori	21-36	26	5	1	5.0
NGC 3293	21-25	23	3	1	3.0
NGC 4755	16-21	17	5	1	5.0
All	16-36	22	13	3	4.3

* Including one very luminous blue giant in I Ori and NGC 3293.

neutrino processes. Their work was later supplemented by further observational and theoretical investigations of the same association along similar lines (Iben 1966*b*; Wildey 1966; Dallaporta and Saggion 1968; Sugimoto *et al.* 1968); additional suggestions have been summarized by Stothers (1969*a*). However, the investigation by Stothers and Chin (1968) shows that the test cannot be made in I Per, because the stars of intermediate mass that are characteristic of the supergiant branches in this association are *red* during a significant part of their helium-burning phase, and are not constantly blue, as earlier models had incorrectly indicated.

The relevant observational data for our purpose here have been abstracted from the tabular information in Stothers (1969*a*) and are summarized in Table 10. The blue/red ratio comparing the numbers of stars (n_b/n_r) is *strictly a lower limit*, because of observational selection effects (as discussed in the earlier paper).

The theoretical results are presented in Table 11 in the form of an *upper limit* to the blue/red ratio of lifetimes (τ_b/τ_r). We have thus assumed that (1) core helium burning occurs *only* in the blue-supergiant region and (2) contraction of the helium core, contraction of the carbon-oxygen core, and carbon burning and later phases occur in the red-supergiant region. The lifetimes in the blue-supergiant region have been taken from Stothers (1969*a*). Now it is required that

$$\tau_b/\tau_r = n_b/n_r . \quad (18)$$

Since $n_b/n_r \geq 5$ (observed) while $\tau_b/\tau_r < 1.7$ without neutrinos and < 17 with neutrinos (theoretical), we may conclude that the weak-interaction neutrino processes provide an adequate explanation for the observed deficiency of M supergiants. Since part of the lifetime during early helium burning will actually occur in the red-supergiant region (Stothers and Chin 1968), the theoretical ratios τ_b/τ_r should be somewhat reduced. This makes our conclusion even stronger.

b) *Statistics of N and S Stars*

The spectra of the most massive red supergiants ($> 20 M_\odot$) ought to show anomalously large abundances of the CNO elements (and presumably some *s*-process elements) after the phase of contraction of the carbon-oxygen core. The best cluster we may use to check this point is I Ori. Here the red supergiant (α Ori) is of spectral type M. Now, as a class, the M stars do not show any obvious anomalies in the CNO elements (Keenan 1963). We may infer that α Ori is probably in the early phase of helium burning or in the phase of contraction of the carbon-oxygen core. By implication, it is likely that most or all of the M supergiants in our sample are in the pre-carbon-burning phase, although at $15 M_\odot$ any observed CNO enrichment would occur only *after* the carbon-burning phase.

TABLE 11
THEORETICALLY PREDICTED UPPER LIMIT ON THE RATIO OF THE NUMBERS
OF BLUE AND RED SUPERGIANTS

M/M_\odot	MAXIMUM LIFE- TIME FOR BLUE REGION τ_b^*	MINIMUM LIFETIME FOR RED REGION τ_r^*		$n_b/n_r = \tau_b/\tau_r$	
		No ν	ν	No ν	ν
15	11.0	5	0.8	2	~ 15
30. . .	5.3	3.5	0.3	1.5	~ 20
60. . . .	3.4	3	0.13	1	~ 25
22.	1.7	~ 17

* Lifetimes are in units of 10^5 years.

Supergiants which may contain the expected abundance anomalies are the rare N and S stars. Although it is uncertain whether any known N or S star is definitely overabundant in the CNO elements (perhaps only the element *ratios* differ from those in M stars), a very massive carbon-burning star would certainly appear as an extreme case of such an object. The carbon stars observed by Mendoza and Johnson (1965) are probably of lower mass than those considered here. The bolometric magnitudes of their stars, although uncertain, range from zero to a maximum brightness of -6 ; a star of $10 M_\odot$ would reach this luminosity at the onset of carbon burning (Iben 1966*a, b*). However, Gordon (1968) has suggested bolometric magnitudes for several N stars as bright as -8 .

A few N and S stars may be associated with very young clusters and associations (Stothers 1969*a*), but their numbers are small in comparison with the numbers of M supergiants. For example, in Stothers's tabulation, thirty-one M supergiants are found while N and S stars are totally absent. More significantly, fifty blue supergiants are found. If it is assumed that a star having the median mass in the tabulation, $15 M_\odot$, evolves under the worst possible circumstances for showing CNO enrichment (by adopting initially a pure carbon core and neglecting silicon-to-iron burning), then the predicted ratio of the lifetime in the blue-supergiant phase to the lifetime in the CNO-enriched phase (neon-to-silicon burning, 0.7×10^5 years) is ≤ 16 without neutrino emission. One would therefore expect to find *at least three* N or S stars (or carbon stars of any

kind) in Stothers's tabulation! Their complete absence is further evidence for the existence of the weak-interaction neutrino processes.

c) Statistics of Yellow Supergiants

The evolutionary phases in which a massive star is expected to cross the Hertzsprung gap occur as follows: (1) radius expansion during the core contraction that follows core hydrogen depletion, (2) radius contraction during the early stages of core helium burning, and (3) radius reexpansion following core helium depletion. These phases ought to be very short. The best time scales available at present are for the first phase. However, fairly reliable time estimates may be made for the other two phases on the basis of the excellent agreement between results of Hofmeister (1967) and Iben (1966*a*) for models of $9 M_{\odot}$ and results of Hayashi and Cameron (1962*a*) and Iben (1966*b*) for models of $15 M_{\odot}$, despite the very different assumptions about initial chemical composition, mixing, opacity, and nuclear-reaction rates. In addition, we have the models of Stothers (1966*a*) for $30 M_{\odot}$. Although not every model sequence makes all three transits across the Hertzsprung gap, each sequence does include the corresponding three evolutionary phases of the interior. On that basis, we may estimate the transit times (to within 30 percent) as if all three transits actually occurred.

It is convenient to express the transit times as percentages of the helium-burning lifetime. Thus, the first crossing requires about 2, 0.5, and <1 percent of the core-helium-burning lifetime for $9 M_{\odot}$, $15 M_{\odot}$, and $30 M_{\odot}$, respectively. For the second crossing, we have only the data for $9 M_{\odot}$, which yields about 3 percent. For the third crossing, the percentages are 10, 2, and <1 percent in order of increasing mass. Summing over all the crossings, we have percentages of 15, ~ 4 , and ~ 1 percent for $9 M_{\odot}$, $15 M_{\odot}$, and $30 M_{\odot}$, respectively. We conclude that massive stars are expected to spend only a small fraction of their post-hydrogen-burning lifetimes in the Hertzsprung gap.

The relative number of yellow supergiants among all the massive supergiants may be obtained from the tabular data in Stothers (1969*a*). If the supergiants in the uncertain I Per "outer" group are excluded, three yellow supergiants are found among fifty-eight blue and red supergiants. The relevant mass range is $10\text{--}35 M_{\odot}$. Additional associations are known to contain yellow supergiants (Schmidt-Kaler 1961), but the number of blue and red members is not known. While the exact percentage of yellow supergiants in our sample may be a little uncertain, it is clear that they do comprise approximately 5 percent of supergiants in the above mass range. This percentage is in good agreement with an averaged theoretical lifetime of 4 percent of the *core-helium-burning* lifetime. It is therefore again indicated that the majority of the observed supergiants (blue and red) are only in the core-helium-burning phase of evolution.

It is useful to point out that two of the above tests—the one involving carbon stars and the other involving yellow supergiants—are independent of the color (blue or red) of the star during the helium-burning phase of evolution.

X. CONCLUSION

Very general models have been constructed for the advanced phases of evolution in massive stars of 15 , 30 , and $60 M_{\odot}$. These masses are representative of evolved supergiants. Independent of the surface condition and the specification of the central energy source, the models may be specified by the two quantities E and T_e . Introduction of the energy source and surface condition shows that the models represent evolutionary sequences of convective red supergiants.

The phases of carbon, neon, and oxygen burning in the stellar core are considered. The latter two phases occur virtually simultaneously. Because of the existing uncertainties in the nuclear-reaction rates of $^{12}\text{C} + \alpha$ and $^{12}\text{C} + ^{12}\text{C}$, two starting core compositions are assumed ($X_{\text{C}} = 1$ and $X_{\text{O}} = 1$) and three rates of the $^{12}\text{C} + ^{12}\text{C}$ reaction are considered. Models are obtained with and without the inclusion of the weak-interaction

neutrino processes (photoneutrinos and pair-annihilation neutrinos). The effects of hydrogen and helium depletion and of moderate rotation are found to be negligible. The possibility of mass loss is also found to be unimportant for our purposes.

During core carbon burning in the star of $15 M_{\odot}$, the core mass increases by a slight amount. Above $\sim 20 M_{\odot}$ and during the later phases of $15 M_{\odot}$, the core evolves with a monotonically decreasing mass due to the growing convective envelope. Thus, in investigating the core evolution of massive red supergiants, we find the widely used assumption of constant mass to be invalid. However, our *instantaneous* core structures agree well with earlier work based on this assumption. Products of the burning of hydrogen, helium, and carbon are mixed to the surface through the hydrogen-burning shell at the base of the envelope. At the onset of the supernova stage, the optical luminosity may be lower than its value on the main sequence (for masses greater than $\sim 30 M_{\odot}$), and the convective envelope is very weakly bound gravitationally in all cases.

Three tests of the hypothesis of electron-neutrino interaction can be made by a comparison of the theoretical evolution times (calculated with and without neutrino emission) with the numbers of massive supergiants in various parts of the H-R diagram of young clusters and associations. A *positive result* is found by using the statistics of M supergiants, N and S stars, and yellow supergiants. These tests seem to be free of the customary ambiguities in interpretation and are positive even when the *maximum* known observational and theoretical uncertainties are applied. Therefore, we conclude that the result of the tests constitutes significant evidence for the existence of the postulated electron-neutrino interaction, in at least the strength required by current theory.

We are deeply grateful to Dr. I. Iben, Jr., for the loan of his computer subroutine to calculate stellar surface conditions and to Dr. J. W. Truran for the loan of his computer program to calculate the products of the carbon-burning reaction. One of us (Chin) gratefully acknowledges a faculty research fellowship for the summer of 1968, administered through the Research Foundation of the State University of New York. It is a pleasure to thank Drs. C. Hayashi, D. Sugimoto, and J. W. Truran for helpful discussions.

REFERENCES

- Allen, C. W. 1963, *Astrophysical Quantities* (London: Athlone Press).
 Arnett, D. W. 1967, *Canadian J. Phys.*, **45**, 1621.
 ———. 1968a, *Ap. J.*, **153**, 341.
 ———. 1968b, *Nature*, **219**, 1344.
 Arnett, W. D., and Truran, J. W. 1969, *Ap. J.*, **157**, 339.
 Bautz, L. P. 1968, *A. J.*, **73**, S4.
 Beaudet, G., and Salpeter, E. E. 1969, *Ap. J.*, **155**, 203.
 Cameron, A. G. W. 1959a, *Ap. J.*, **130**, 429.
 ———. 1959b, *ibid.*, **130**, 895.
 Chiu, H.-Y. 1961, *Ann. Phys.*, **15**, 1.
 ———. 1963, *A. J.*, **68**, 70.
 ———. 1966, *Ann. Rev. Nucl. Sci.*, **16**, 591.
 Colgate, S. A. 1968, *Ap. J.*, **153**, 335.
 Colgate, S. A., and White, R. H. 1966, *Ap. J.*, **143**, 626.
 Dallaporta, N., and Saggion, A. 1968, *Pub. Osservatorio Astr. Padova*, No. 148.
 Deinzer, W., and Salpeter, E. E. 1965, *Ap. J.*, **142**, 813.
 Deutsch, A. J. 1956, *Ap. J.*, **123**, 210.
 Faulkner, D. J. 1968, *M.N.R.A.S.*, **140**, 223.
 Forbes, J. E. 1968, *Ap. J.*, **153**, 495.
 Fowler, W. A., Caughlan, G. R., and Zimmerman, B. A. 1967, *Ann. Rev. Astr. and Ap.*, **5**, 525.
 Fowler, W. A., and Hoyle, F. 1964, *Ap. J. Suppl.*, **9**, 201.
 Fraley, G. S. 1968, *Ap. and Space Sci.*, **2**, 96.
 Gabriel, M., and Noels-Grötsch, A. 1968, *Ann. d'ap.*, **31**, 167.
 Gordon, C. P. 1968, *Pub. A.S.P.*, **80**, 597.
 Hayashi, C. 1966, in *Stellar Evolution*, ed. R. F. Stein and A. G. W. Cameron (New York: Plenum Press), p. 253.

- Hayashi, C., and Cameron, R. C. 1962*a*, *Ap. J.*, **136**, 166.
 ———. 1962*b*, *A.J.*, **67**, 577.
 ———. 1964, *ibid.*, **69**, 140.
 Hayashi, C., Hōshi, R., and Sugimoto, D. 1962, *Progr. Theoret. Phys. Suppl.* (Kyoto), No. 22.
 Hofmeister, E. 1967, *Zs. f. Ap.*, **65**, 164.
 Iben, I., Jr. 1963, *Ap. J.*, **138**, 452.
 ———. 1966*a*, *ibid.*, **143**, 505.
 ———. 1966*b*, *ibid.*, **143**, 516.
 Keenan, P. C. 1963, in *Basic Astronomical Data*, ed. K. Aa. Strand (Chicago: University of Chicago Press), p. 78.
 Kippenhahn, R., Thomas, H.-C., and Weigert, A. 1966, *Zs. f. Ap.*, **64**, 373.
 Kutter, G. S., and Savedoff, M. P. 1967, *A.J.*, **72**, 811.
 Loebenstein, H. M., Mingay, D. W., Winkler, H. C., and Zaidins, C. S. 1967, *Nucl. Phys.*, **A91**, 481.
 Masani, A., Borghese, P., Ferrari, A., and Gallino, R. 1968, *Ann. d'ap.*, **31**, 367.
 Masani, A., Gallino, R., and Silvestro, G. 1965, *Nuovo Cimento*, **38**, 1142.
 Masevich, A. G., Kotok, E. V., Dluzhnevskaya, O. B., and Masani, A. 1965, *Astr. Zh.*, **42**, 334.
 Mendoza, E. E., and Johnson, H. L. 1965, *Ap. J.*, **141**, 161.
 Murai, T., Sugimoto, D., Hōshi, R., and Hayashi, C. 1968, *Progr. Theoret. Phys.* (Kyoto), **39**, 619.
 Noels-Grötsch, A., Boury, A., and Gabriel, M. 1967, *Ann. d'ap.*, **30**, 13.
 Paczynski, B., and Ziolkowski, J. 1968, *Acta Astr.*, **18**, 255.
 Rakavy, G., Shaviv, G., and Zinamon, Z. 1967, *Ap. J.*, **150**, 131.
 Reeves, H. 1962, *Ap. J.*, **135**, 779.
 ———. 1963, *ibid.*, **138**, 79.
 ———. 1965, in *Stellar Structure*, ed. L. H. Aller and D. B. McLaughlin (Chicago: University of Chicago Press), p. 113.
 Reeves, H., and Salpeter, E. E. 1959, *Phys. Rev.*, **116**, 1505.
 Rose, W. K. 1969, *Ap. J.*, **155**, 491.
 Schmidt-Kaler, T. 1961, *Zs. f. Ap.*, **53**, 128.
 Schwarzschild, M. 1958, *Structure and Evolution of the Stars* (Princeton, N.J.: Princeton University Press).
 Stephenson, G. J., Jr. 1966, *Ap. J.*, **146**, 950.
 Stothers, R. 1963*a*, *Ap. J.*, **137**, 770.
 ———. 1963*b*, *ibid.*, **138**, 1074.
 ———. 1964, *ibid.*, **140**, 510.
 ———. 1965, *ibid.*, **141**, 671.
 ———. 1966*a*, *ibid.*, **143**, 91.
 ———. 1966*b*, *ibid.*, **144**, 959.
 ———. 1969*a*, *ibid.*, **155**, 935.
 ———. 1969*b*, *ibid.*, **156**, 541.
 Stothers, R., and Chin, C.-W. 1968, *Ap. J.*, **152**, 225.
 Sugimoto, D., Yamamoto, Y., Hōshi, R., and Hayashi, C. 1968, *Progr. Theoret. Phys.* (Kyoto), **39**, 1432.
 Takarada, K., Sato, H., and Hayashi, C. 1966, *Progr. Theoret. Phys.* (Kyoto), **36**, 504.
 Truran, J. W., Cameron, A. G. W., and Gilbert, A. 1966, *Canadian J. Phys.*, **44**, 563.
 ———. 1968, *ibid.*, **46**, 1019.
 Tsuda, H. 1963, *Progr. Theoret. Phys.* (Kyoto), **29**, 29.
 Weigert, A. 1966, *Zs. f. Ap.*, **64**, 395.
 Weymann, R. 1962, *Ap. J.*, **136**, 844.
 Wildey, R. L. 1966, in *Colloquium on Late-Type Stars*, ed. M. Hack (Astronomical Observatory of Trieste), p. 405.
 Wilson, O. C. 1960, *Ap. J.*, **131**, 75.

